Jurnal Geologi dan Sumberdaya Mineral
Journal of Geology and Mineral Resources
Center for Geological Survey, Geological Agency, Ministry of Energy and Mineral Resources
Journal homepage: http://jgsm.geologi.esdm.go.id
ISSN 0853 - 9634, e-ISSN 2549 - 4759

Preliminary Result on Optimum Seed Generation Bandwidth for Object-Based Image Segmentation (OBIS) of Porphyritic Igneous Thin Sections

Hasil Pendahuluan Optimum Generation Bandwidth untuk Segmentasi Citra Berbasis Objek pada Sayatan Tipis Batuan Beku Porfiritik

Rio Priandri Nugroho[1], Victoria Vania Blanca Widjaya[1], and Mohamad Roviansah[2]

[1]Universitas Pertamina

[2]PT Aria Agri Indonesia

email: rio.priandri@universitaspertamina.ac.id

Naskah diterima: 02 Juni 2022, Revisi terakhir: 19 Januari 2024, Disetujui: 19 Januari 2024 Online: 21 Februari 2024
DOI: http://dx.doi.org/10.33332/jgsm.geologi.v25i1.698

Abstract-Crystal size distribution (CSD) analysis is one of many methods for studying the crystallization history of magma. It involves labor-intensive digitation of all crystals, which may prolong the processing of large data sets. This study presents a preliminary result of Object-Based Image Segmentation (OBIS) as a semi-automatic approach in crystal digitation. Five data sets containing 9 photomicrographs of porphyritic igneous rock thin sections were processed using SAGA GIS. The procedure produced an optimum bandwidth equation of y = 38.455 ln(x) + 114, where x is the average size of sampled crystal in mm. Segmentation tests on another sample using the formula returned good and consistent results with important notes on sensitivity to textures which may result in crystal segment separation, such as fractures, veins, and sieve, as well as the inability to separate all groundmass crystals. Even though it shows good results, this formula only applies where the pixel-to-length conversion factor of 562.2 pixel/mm.

Keywords: OBIS, SAGA GIS, Optimum bandwidth, Photomicrograph, Porphyritic igneous rock thin section.

Abstrak-*Analisis distribusi ukuran kristal (crystal size distribution, CSD) adalah salah satu metode studi sejarah kristalisasi magma. Metode ini melibatkan digitasi seluruh kristal yang dapat memperlambat pengolahan data set berukuran besar. Pada studi ini, disajikan hasil pendahuluan Object-Based Image Segmentation (OBIS) sebagai pendekatan semi-otomatis dalam digitasi kristal. Lima data set yang masing-masing terdiri dari 9 foto mikrograf sayatan tipis batuan beku porfiritik, diproses menggunakan SAGA GIS. Prosedur tersebut menghasilkan persamaan bandwidth optimal y = 38,455 ln(x) + 114 dengan x adalah ukuran rata-rata sampel kristal dalam mm. Uji segmentasi pada sampel lain menggunakan persamaan tersebut membuahkan hasil yang baik dan konsisten dengan catatan penting pada sensitivitas terhadap tekstur yang dapat menghasilkan pemisahan segmen kristal seperti rekahan, urat, dansieve, serta ketidak mampuan memisahkan seluruh kristal massa dasar. Akan tetapi, persamaan ini hanya berlaku pada foto mikrograf dengan faktor konversi piksel-kepanjang sebesar 562,2 piksel/mm.*

Katakunci*: OBIS, SAGA GIS, Bandwidth optimum, Foto mikrograf, Sayatan tipis batuan beku porfiritik.*

INTRODUCTION

Crystal Size Distribution (CSD) is a method to quantitatively study the crystallization history of magma (e.g. Cashman and Ferry, 1988; Fornaciai *et al*., 2015; Higgins, 1996; Klein *et al.*, 2018; Moschini *et a*l., 2021; Nugroho *et al*., 2019; Zhang *et al.*, 2019). The conventional way of conducting this method is by manually digitizing targeted crystals in an image manipulation program, then processing them in ImageJ (Schneider *et al*., 2012), or digitizing and processing them directly in ImageJ. With the advancement of computing, processing the extracted crystal sizes is a relatively easy step. However, manual digitation of the thin section photomicrographs is still labor-intensive, especially when dealing with large data sets. To tackle that issue, this paper presents a preliminary result of optimum seed generation bandwidth used in Object-Based Image Segmentation (OBIS) (Adams and Bischof, 1994; Bechtel et al., 2008) of SAGA GIS (Conrad *et al.*, 2015) to digitize plagioclase crystals from thin-section photomicrographs. It will be a puzzle piece in larger research towards semi-automatic CSD analysis.

DATA

The data used in this study are five sets of thin-section photomicrographs (Figure 1) with porphyritic texture taken from Kebo-Butak Formation located in KulonProgo, Yogyakarta. Rocks with porphyritic texture were chosen to obtain optimum seed generation bandwidths for various crystal sizes, which are common in igneous rocks, especially in volcanic rocks. In addition, porphyritic igneous rocks are commonly processed using manual CSD to produce magma residence time and to predict the magma dynamics. The petrographic properties of each sample are presented in Table 1.

Each set of porphyritic rocks photomicrograph contains 9 images that were taken with these configurations: plane-polarized light (PPL), cross-polarized light (XPL), XPL with gypsum plate, XPL with analyzer orientation of 15°, 30°, 45°, 60°, 75°, and 90° (Figure 2). This configuration was used to identify minerals with polyphase characteristics (Asmussen *et al*., 2015). The images were taken on 4x objective magnification and 1920 x 1080 pixel output setting. Pixel to length calibration factor for each image is 562.2 pixel/mm. For validation, an image set from the same sample was taken.

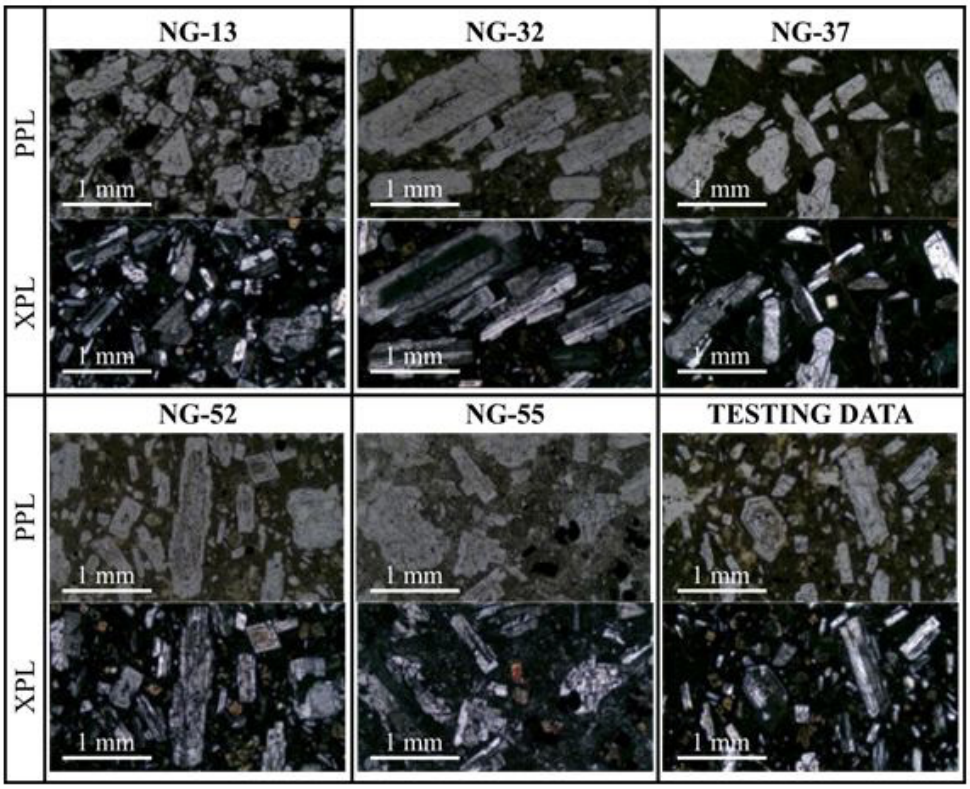

Fig. 1. Data sets used in this study were inplane-polarized (PPL; upper image of each sample) and cross-polarized(XPL; lower image of each sample) views.

Table 1. Petrographic features of samples used in this study.

No	Sample Code	Rock Type	Petrographic Features
1	NG-13	Andesite	Hypocrystalline, porphyritic with phenocryst of plagioclase (0.23-0.90 mm, prismatic, euhedral-subhedral, some are fractured, with sieve texture) and opaque mineral, with groundmass of plagioclase microlith and glass. Secondary minerals observed are calcite (filling cracks in plagioclase) and chlorite (disseminated).
2	NG-32	Andesite	Hypocrystalline, porphyritic with phenocryst of plagioclase (0.23-2.1 mm, prismatic, euhedral-subhedral, with sieve texture and compositional zoning, mostly fractured), hornblende (0.11-0.23 mm, prismatic, subhedral), and opaque mineral, with groundmass of plagioclase microliths and glass. Secondary minerals observed are calcite (filling cracks in plagioclase) and chlorite (disseminated).
3	NG-37	Andesite	Hypocrystalline, porphyritic with phenocryst of plagioclase (0.23-1.63 mm, prismatic, euhedral-subhedral, with sieve texture, some are fractured), clinopyroxene (0.23-0.46 mm, prismatic, anhedral-subhedral), and opaque mineral, with groundmass of plagioclase microliths and glass. Secondary minerals observed are calcite (filling cracks in plagioclase and veins) and chlorite (disseminated).
4	NG-52	Andesite	Hypocrystalline, porphyritic with phenocryst of plagioclase (0.23-1.63 mm, prismatic, euhedral-subhedral, with sieve texture and compositional zoning, some are fractured), hornblende (0.11-0.3 mm, prismatic, subhedral), and opaque mineral, with groundmass of plagioclase microliths and glass. Secondary minerals observed are calcite (filling cracks in plagioclase) and chlorite (disseminated).
5	NG-55	Andesite	Hypocrystalline, porphyritic with phenocryst of plagioclase (0.23-2 mm, prismatic, euhedral-subhedral, mostly fractured), clinopyroxene (0.11-0.35 mm, prismatic, euhedral), and opaque mineral, with groundmass of plagioclase microliths and glass. Secondary minerals observed are calcite (filling cracks in plagioclase) and chlorite (disseminated).
6	TESTING DATA	Andesite	Hypocrystalline, porphyritic with phenocryst of plagioclase (0.23-1.63 mm, prismatic, euhedral-subhedral, with sieve texture and compositional zoning, some are fractured), hornblende (0.11-0.35 mm, prismatic, subhedral), and opaque mineral, with groundmass of plagioclase microliths and glass. Secondary minerals observed are calcite (filling cracks in plagioclase) and chlorite (disseminated).

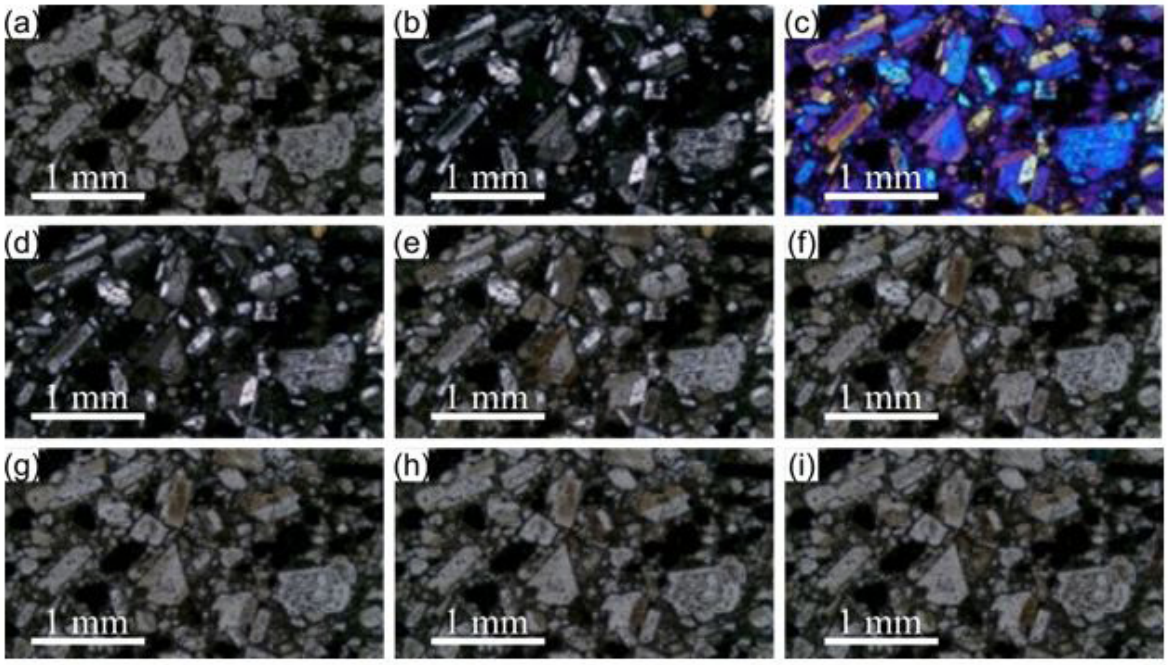

Figure 2. Example data set from sample NG-13; (a) PPL; (b) XPL; (c) XPL with gypsum plate; XPL with analyzer orientation of (d) 15°, (e) 30°, (f) 45°, (g) 60°, (h) 75°, and (i) 90°.

METHODOLOGY

Object-Based Image Segmentation

This study uses SAGA GIS (Conrad *et al.*, 2015), a free and open-source geographic information system software. Previous authors have used this software to process thin-section photomicrograph data using its image-processing tools (e.g. Asmussen *et al.*, 2015; Kölln *et al*., n.d.). Object-Based Image Segmentation tools with the von Neumann algorithm were used to create polygons delineating plagioclase crystals for this research. The segmentation was conducted in the three-part subsequent iteration.

Segmentation of phenocryst

Segmentation of phenocryst was conducted with bandwidth multiplication of 50, which are 50, 100, 150, and 200. The result of two bandwidths with the best fit among those four was later resegmented with a bandwidth multiplication 10. For example, if the best two are 100 and 150, the bandwidth for the subsequent trial will be 110, 120, 130, and 140. The segment with the best fit from this trial was then used to prepare data for the next iteration. Polygons containing phenocryst crystals were extracted, and the rest of the polygons were merged. The merged polygon was used to clip the input photomicrographs to produce phenocryst-free image sets for the next iteration.

Segmentation of microphenocryst

Segmentation of micro phenocryst was conducted using the phenocryst-free image sets with bandwidth multiplication of 10, which are 10, 20, 30, 40, and 50. The result of two bandwidths with the best fit among those five was later resegmented with a bandwidth multiplication of 5. For example, if the best two are 40 and 50, the bandwidth for the subsequent trial will be 45. The segment with the best fit from this trial was then used to prepare data for the groundmass iteration. Polygons containing microphenocryst crystals were extracted, and the rest of the polygons were merged. The merged polygon was used to clip the input photomicrographs to produce the groundmass-only image for the next iteration.

Segmentation of groundmass

Segmentation of groundmass was conducted using the groundmass-only image sets. For this segmentation, only PPL and XPL images were used to minimize confusion in small objects due to the large variation introduced by the other 7 images. Bandwidth multiplication of 1 from 1 until 10 was used in this segmentation. The best result with the best fit the used for calculation.

Manual Image Digitation

To acquire real dimensional data of the crystals, manual digitation of plagioclase from each size class was conducted. The digitation and processing of the plagioclase were conducted using a SAGA GIS segment digitizer and polygon shape indices tools. The polygon shape indices tool extracts the length of the digitized crystals. Pixel to length conversion value of 562.2 pixel/mm was used to convert the calculated pixel to the actual size. The average value of each crystal population from all samples was later calculated. These values were used later in bandwidth-to-length correlation.

Bandwidth to Length Correlation

The correlation between the optimum bandwidth and the average length was calculated by plotting the values of each sample on an x-y graph. A regression line was later drawn, and a correlation equation was calculated. This formula was later used to test the segmentation bandwidth in another sample.

Regression Equation Testing

The calculated regression equation was put tothe test. Test image sets were digitized manually to obtain a polygon representing each size class. The length of the crystals for each size class was converted and used to calculate the optimum bandwidth for segmentation. The segmentations were later conducted using calculated values following the phenocryst-microphenocryst-groundmass segmentation procedure mentioned before.

Validation

Validation of the procedures was conducted qualitatively. Qualitative validation was done by observing how individual crystals were segmented. In OBIS, a single object might be separated into several segments if the object has visually significant discontinuities, such as cracks or fractures. This observation was conducted on both sample populations; on the original five data sets and the testing data set. Observation of separation was done to see whether a consistent pattern was present.

The whole process of this study is available as a flowchart in Figure 3.

RESULT OF STUDY

Initial Segmentation

The optimum bandwidths are obtained from segmentation iterations for all size populations of all samples. It can be seen in Table 2 that variation is present for eachsize class. However, the optimum bandwidth for each size class still lies on similar values. An example of segmentation from Sample NG-13 can be seen in Figure 4, Figure 5, and Figure 6.

The iterations produce segments with good crystal delineation. However, some crystals are separated into more than one segment. The phenocrysts are commonly separated into 4-5 segments for each crystal (e.g.,Figure 7), while the microphenocrysts and groundmasses are separated into 2 segments for each crystal. Phenocryst and microphenocryst crystals are commonly separated along fractures or cleavages (Figure 4, Figure 5, and Figure 7), which were previously described in Table 1. However, some groundmass crystals are clumped together (Figure 6).

Manual digitation of all size classes was conducted using SAGA GIS. Using the algorithm, the average length in pixels was also calculated. Conversion from pixel to mm returned values, as seen in Table 3.

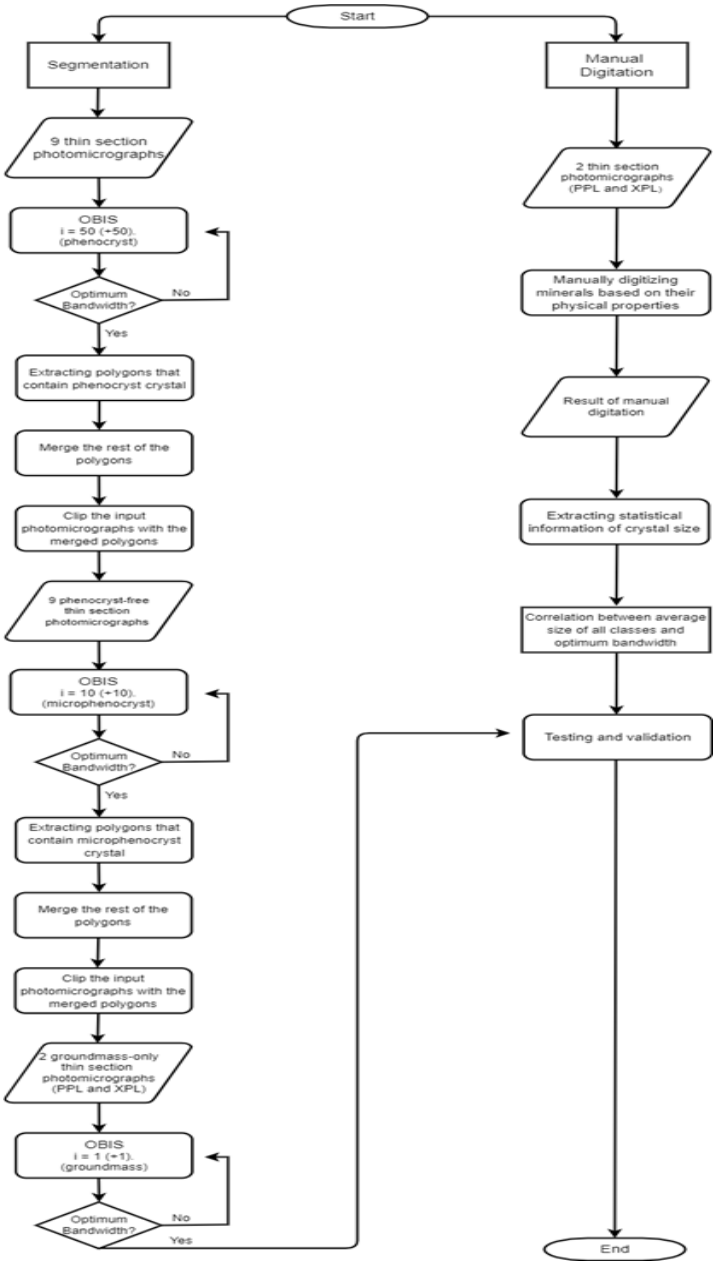

Figure 3. Flowchart showing the whole process in this study.

Table 2. Optimum bandwidth for all crystal size classes from each sample.

Sample Code	Optimum Bandwidth		
	Phenocryst	Microphenocryst	Groundmass
NG-13	110	50	10
NG-32	120	50	5
NG-37	130	50	10
NG-55	100	50	10
NG-57	110	35	5

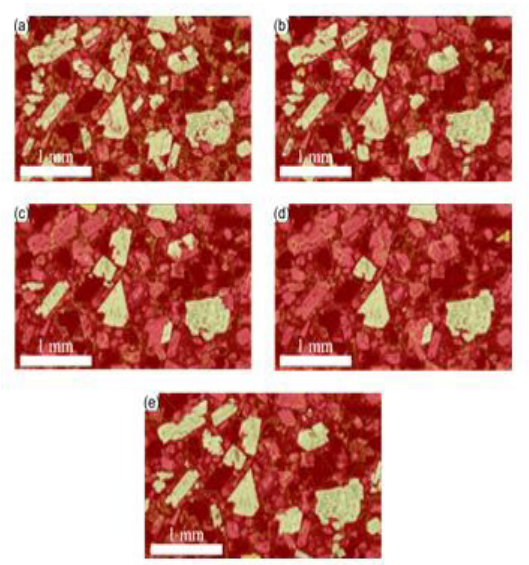

Figure 4. Crossed polarized images that show example of phenocryst segmentation from sample NG-13 with different bandwidths; (a) 50; (b) 100; (c) 150; (d) 200; (e) optimum bandwidth of 110. The yellow-colored area represents phenocryst, and the yellow lines represent segment boundaries.

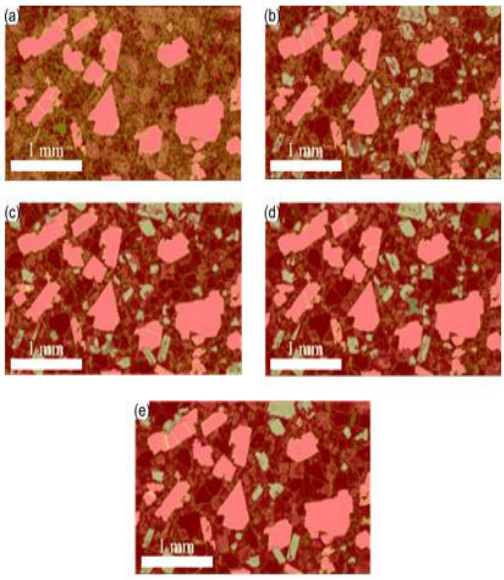

Figure 5. Crossed polarized images that show example of microphenocryst segmentation from sample NG-13 with different bandwidths; (a) 10; (b) 20; (c) 30; (d) 40; (e) optimum bandwidth of 50. Yellow-coloredareas represent phenocrysts, and yellow lines represent segment boundaries.

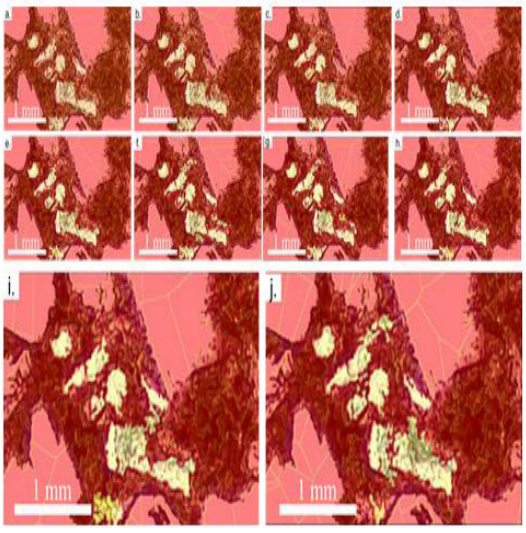

Figure 6. Crossed polarized images that show example of groundmass segmentation from sample NG-13 with different bandwidths; (a) 1; (b) 2; (c) 3; (d) 4; (e) 5; (f) 6; (g) 7; (h) 8; (i) 9; and (j) optimum bandwidth of 10. The yellow-colored area represents phenocryst, and the yellow lines represent segment.

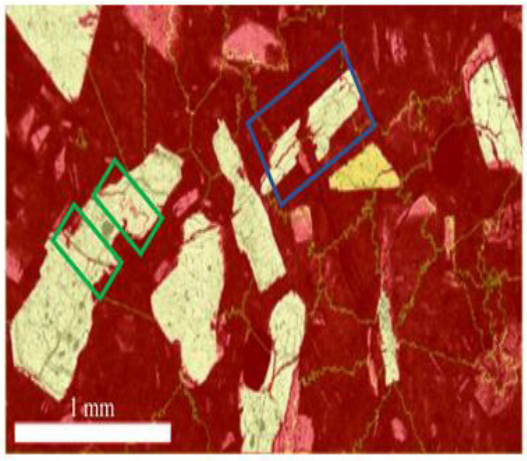

Figure 7. Crossed polarized image segmentation of NG-37 with a bandwidth of 130 shows mineral separation due to the occurrence of veins (blue box) and fractures (green box).

Table 3. Average crystal size for all size classes from each sample. Abbreviations are S – sieve; F – fracture; V – vein; Z: compositional zoning; N/O – not observed.

Sample Code	Avg (mm)	Max (mm)	Min (mm)	Std Dev (mm)	Optimum Bandwidth	Observed Feature(s)
Phenocryst						
NG-13	0.639	0.854	0.517	0.129	110	S, F
NG-32	1,643	2,297	1,252	0.57	120	S, F, Z
NG-37	0.751	1,363	0.519	0.286	130	S, F, V
NG-52	0.914	1,611	0.632	0.331	100	S, F, Z
NG-55	0.772	1,212	0.531	0.259	110	F
Microphenocryst						
NG-13	0.202	0.445	0.1	0.087	50	S, F
NG-32	0.182	0.492	0.1	0.097	50	S, F, Z
NG-37	0.217	0.457	0.1	0.11	50	S, F, V
NG-52	0.179	0.437	0.1	0.084	50	S, F, Z
NG-55	0.196	0.405	0.1	0.089	35	F
Groundmass						
NG-13	0.061	0.099	0.023	0.022	10	N/O
NG-32	0.052	0.094	0.017	0.021	5	N/O
NG-37	0.064	0.094	0.042	0.015	10	N/O
NG-52	0.056	0.098	0.014	0.024	10	N/O
NG-55	0.071	0.099	0.035	0.018	5	N/O

The average size of all classes and corresponding optimum bandwidth data, as presented in Table 3,were plotted on an x-y graph (Figure 8). The dashed line in Figure 8 represents the regression line of the plotted data. From the regression, the optimum bandwidth for a given average size is shown by Equation 1.

$$y = 38.455 \ln(x) + 114 \quad (1)$$

y: optimum bandwidth

x: average size

Testing and Validation

Testing of the equation was conducted on one sample. Calculations of optimum bandwidth from measured crystal samples are presented in Table 4. Then, the optimum bandwidth values were used for iterations like those of the first five samples. From the iteration, the segments delineate some crystals' shapes with a good fit. However, the separation of crystal segments still occurred (Figure 9). The phenocrysts are commonly separated into 4 segments for each crystal, while the microphenocrysts are separated into 3 segments for each crystal. For the groundmasses, separation of 2-4 segments is observed. In the case of phenocryst and microphenocryst, separation occurred along discontinuities within crystals, such as fractures and cleavages (Figure 9), which was previously described in Table 1. Similar to the initial segmentation result, some groundmass crystals are clumped.

DISCUSSION

From the procedure described above, it can be seen that OBIS is able to delineate plagioclase of igneous thin sections with porphyritic texture. This procedure must use different bandwidths for each class size. Bandwidth too big will result in clumping different objects, while bandwidth too small will separate single objects into many small segments.

The correlation equation between average crystal size and optimum bandwidth, as shown in Equation 1, produced good delineation with object separation. It should be noted that the equation can only be applied to a photomicrograph with the same pixel to the length conversion factor. In addition, groundmass crystal clumping, as shown in initial segmentation and testing, indicates that the semi-automatic segmentation procedure has a lower crystal size limit in pixels that cannot separate individual crystals.

In the case of crystal separation, it might be caused by crystal fractures that have been observed before segmentation (Table 1). Fractures may be filled by the material of different properties (e.g., glass or crystal groundmass) that separates the fragments. Another explanation is that fractures may cause crystal fragments to rotate, which results in two grains of different optical orientations. In addition, crystal separation also occurs in crystals with mesh in their zonation, which has a significant difference in optical properties due to groundmass filling. Hence, this procedure is sensitive to rock or crystal textures that should be mitigated by careful manual editing.

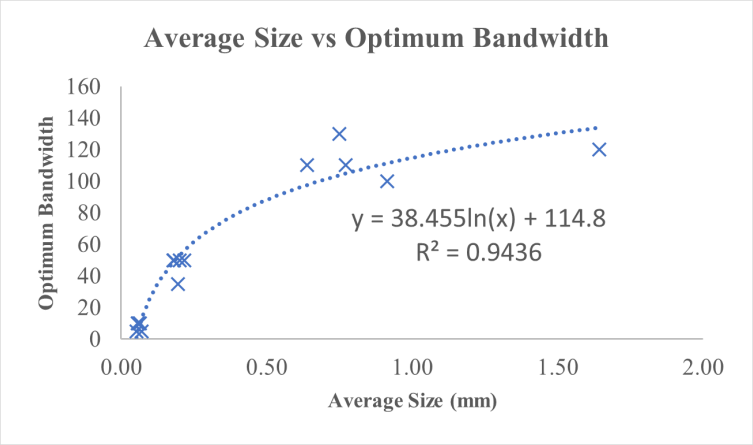

Figure 8. Correlation between average size and optimum bandwidth from five samples.

Table 4. Optimum bandwidth of tested thin section.

Size Class	Average size (mm)	Optimum Bandwidth
Phenocryst	0.743	103,377
Microphenocryst	0.23	582,836
Groundmass	0.087	208,988

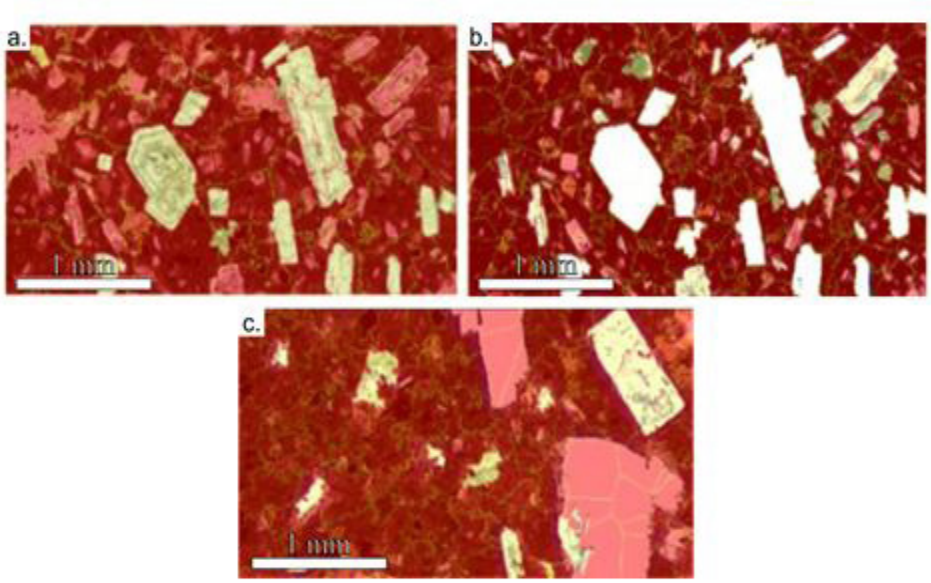

Figure 9. Crossed polarized images that show phenocryst segmentation testing result with bandwidth calculated using Equation 1; (a) phenocryst; (b) microphenocryst; (c) groundmass.

CONCLUSION

These are the conclusion of this study:

- OBIS shows a capability to delineate crystals of different sizes in porphyritic thin igneous sections.
- The optimum bandwidth equation calculated in this study (y = 38.455 ln(x) + 114) produces good segments for images with the same pixel-to-length conversion factor.
- OBIS shows limitations in separating groundmass crystals due to their size.
- OBIS has a sensitivity to rocks or crystal textures, such as fractures, veins, and sieves, which result in crystal separation.

ACKNOLEDGEMENT

Authors are thankful to anonymous reviewers for their input in the review of this paper.

REFERENCES

Adams, R., Bischof, L., 1994. Seeded region growing. IEEE Trans. Pattern Anal. Mach. Intell. 16, 641–647.

Asmussen, P., Conrad, O., Günther, A., Kirsch, M., Riller, U., 2015. Semi-automatic segmentation of petrographic thin section images using a "seeded-region growing algorithm" with an application to characterize wheathered subarkose sandstone. Comput. Geosci. 83, 89–99. https://doi.org/10.1016/j.cageo.2015.05.001

Bechtel, B., Ringeler, A., Böhner, J., 2008. Segmentation for Object Extraction of Trees using MATLAB and SAGA. SAGA–Seconds Hambg. Beitr. Zur Phys. Geogr. Landschaftsökologie Univ Hambg. Inst Für Geogr. 1–12.

Cashman, K.V., Ferry, J.M., 1988. Crystal size distribution (CSD) in rocks and the kinetics and dynamics of crystallization: III. Metamorphic crystallization. Contrib. Mineral. Petrol. 99, 401–415.

Conrad, O., Bechtel, B., Bock, M., Dietrich, H., Fischer, E., Gerlitz, L., Wehberg, J., Wichmann, V., Böhner, J., 2015. System for automated geoscientific analyses (SAGA) v. 2.1. 4. Geosci. Model Dev. 8, 1991–2007.

Fornaciai, A., Perinelli, C., Armienti, P., Favalli, M., 2015. Crystal size distributions of plagioclase in lavas from the July–August 2001 Mount Etna eruption. Bull. Volcanol. 77, 1–15.

Higgins, M.D., 1996. Magma dynamics beneath Kameni volcano, Thera, Greece, as revealed by crystal size and shape measurements. J. Volcanol. Geotherm. Res. 70, 37–48. https://doi.org/10.1016/0377-0273(95)00045-3

Klein, J., Mueller, S.P., Helo, C., Schweitzer, S., Gurioli, L., Castro, J.M., 2018. An expanded model and application of the combined effect of crystal-size distribution and crystal shape on the relative viscosity of magmas. J. Volcanol. Geotherm. Res. 357, 128–133.

Kölln, S., Conrad, O., Riller, U., n.d. Quantification of the fractal dimension of cataclasites in granitoid target rocks of the Chicxulub impact crater (Yucatán peninsula, Mexico) using SAGA GIS image analysis.

Moschini, P., Mollo, S., Gaeta, M., Fanara, S., Nazzari, M., Petrone, C.M., Scarlato, P., 2021. Parameterization of clinopyroxene growth kinetics via crystal size distribution (CSD) analysis: Insights into the temporal scales of magma dynamics at Mt. Etna volcano. Lithos 396–397, 106225. https://doi.org/10.1016/j.lithos.2021.106225

Nugroho, R.P., Disando, T., Kurniawan, I.A., Abdurrachman, M., 2019. Crystal size distribution (CSD) of plagioclase phenocryst-microphenocryst and the calculation of crystal resident times in the continuous central eruption sequences of Mount Lasem, Central Java, Indonesia. J. Phys. Conf. Ser. 1363, 012041. https://doi.org/10.1088/1742-6596/1363/1/012041

Schneider, C.A., Rasband, W.S., Eliceiri, K.W., 2012. NIH Image to ImageJ: 25 years of image analysis. Nat. Methods 9, 671–675. https://doi.org/10.1038/nmeth.2089

Zhang, B., Hu, X., Asimow, P.D., Zhang, X., Xu, J., Fan, D., Zhou, W., 2019. Crystal size distribution of amphibole grown from hydrous basaltic melt at 0.6–2.6 GPa and 860–970 C. Am. Mineral. 104, 525–535.